*J Mater Sci* (2017) 52:12553–12573

Review

# Determination of material properties of thin films and coatings using indentation tests: a review

Wu Wen[1], Adib A. Becker[1,*], and Wei Sun[1]

[1] *Faculty of Engineering, University of Nottingham, University Park, Nottingham NG7 2RD, UK*

**Received:** 5 April 2017
**Accepted:** 4 July 2017
**Published online:** 17 July 2017



## ABSTRACT

This paper presents a review of the mechanical characterisation of thin film and coated systems using indentation tests. The potential in assessing mechanical properties of films and coatings using indentation tests has received a great deal of attention since this knowledge is vital for predicting their performance. The relevant theoretical background is discussed. Experimental work, numerical studies and data interpretation techniques for indentation on single bulk materials and thin films are discussed. Surface conditions, indentation depths and indentation size effects for indentation tests on thin films and coated systems are discussed. Data interpretation methods for indentation on films and coated systems are reviewed with a discussion on their limitations. Other studies in this field concerning the substrate effects and critical indentation depth ratios are also discussed. Suggestions for future experimental work and data interpretation are provided.

## Introduction

Indentation tests have been widely used for mechanical characterisation of single bulk materials and coated systems. Generally, a small sharp indenter penetrates a material test piece within a certain force or displacement range, by which they are categorised into three types: macro-indentation, micro-indentation and nano-indentation. This non-destructive test method has the advantages of being able to provide information related to local near-surface mechanical properties of the test piece. This is especially important for thin films and coated systems since it is critical to separate the mechanical properties of the film and coating from the system. In recent decades, a number of experiments, e.g. [1–19], and numerical simulations, e.g. [2–13], have been carried out to obtain displacement and load responses of many different bulk materials and coated systems. The load–displacement curves obtained from experiments and simulations are the main data used for the analysis. Other outputs include the surface profile and the stress and strain distributions. The main focus of data interpretation has been to extract mechanical properties of the bulk materials or the films and coatings, such as Young's modulus, yield strength, Poisson's ratio and work-hardening exponent for power law materials. Many analyses of indentation tests are based on the classic indentation theory developed by Olive and Pharr [1]. Different

Address correspondence to E-mail: a.a.becker@nottingham.ac.uk

DOI 10.1007/s10853-017-1348-3

data interpretation methods for bulk materials [20–33] and thin film or coatings [34–36] have been proposed over the years. Usually, these methods involve dimensional analysis or inverse analysis using FE analysis (FEA).

Determining the mechanical properties of coatings is more challenging compared to single bulk material due to the effects of the substrate and indentation size effect. A review of the analysis and interpretation of nano-indentation tests discussing the common errors in using the indentation technique has been published by Fischer-Cripps [37]. The focus of that review is pointing out the possible mistakes and sources of error for the practitioners and provides a guidance for necessary correlations. The discussion on extracting material properties is limited to elastic modulus and hardness. This present work aims to provide a comprehensive review of mechanical characterisation of thin films and coated systems using indentation tests from most aspects, including theoretical studies, experiments and numerical studies. Regarding the determination of mechanical properties, elastoplastic properties, i.e. Young's modulus, Poisson's ratio, the yield stress and the work-hardening exponent, are included. The developments and limitations of certain existing methods of determining the mechanical properties of materials using indentation tests are reviewed.

## Theoretical studies

### Classic indentation theory

To relate the mechanical properties of materials to indentation load–displacement data, there have been several theoretical studies, with the focus on the elastic modulus, E, and hardness, H. The classic theory of Oliver and Pharr [1] is the most commonly used one. Basically, the load ($P$) is described as a function of displacement ($h$). A typical $P$–$h$ curve of an elastoplastic material from an indentation test is shown in Fig. 1. The $P$–$h$ curve from the loading process can be described by Kick's Law,

$$P = Ch^2 \tag{1}$$

where $C$ is the loading curve curvature. Oliver and Pharr's theory relates the measured initial unloading contact stiffness, $S = \mathrm{d}P/\mathrm{d}h$, to Young's modulus, $E$, of the test material. This relationship is given by

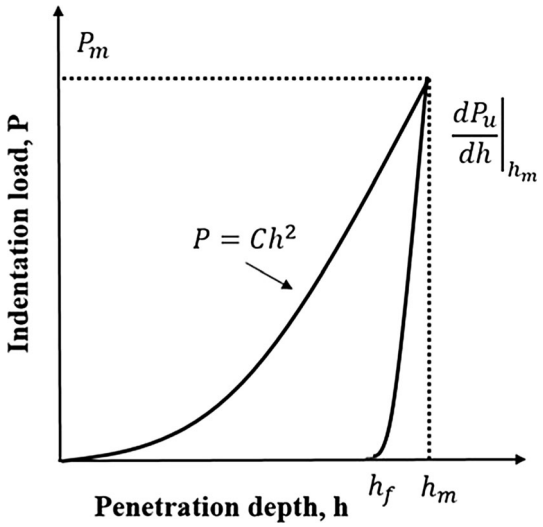


**Figure 1** Schematic illustration of a typical $P$–$h$ response of an elastoplastic material to instrumented indentation. Reproduced from [1] with permission from Cambridge University Press.

$$S = \left(\frac{\mathrm{d}P}{\mathrm{d}h}\right)_{hm} = \frac{2}{\sqrt{\pi}} E_\mathrm{r}\sqrt{A} \tag{2}$$

where $(\mathrm{d}P/\mathrm{d}h)_{\mathrm{hm}}$ is the unloading slope at the maximum displacement $h_\mathrm{m}$, $E_\mathrm{r}$ is the reduced modulus and is defined as follows

$$\frac{1}{E_r} = \frac{1-v_i^2}{E_i} + \frac{1-v^2}{E} \tag{3}$$

where $v$, $E$, $v_i$, $E_i$ are Poisson's ratio and Young's modulus of the test material and indenter, respectively. $A$ is the projected contact area at the maximum load, $A = \pi a^2$, where $a$ is the contact radius as shown in Fig. 2. The approach above has been suggested to be applicable to any indenter that can be described as a body of revolution of a smooth function [38]. For non-axisymmetric polygonal indenters, such as Vickers and Berkovich indenters, a correction factor $\beta$ can be introduced to Eq. (2) [38]:

$$S = \frac{\mathrm{d}P}{\mathrm{d}h} = \beta\frac{2}{\sqrt{\pi}} E_\mathrm{r}\sqrt{A} \tag{4}$$

where $\beta = 1.034$ for a Berkovich indenter and $\beta = 1.024$ for a Vickers indenter. The hardness of the test material can be easily calculated from:

$$H = \frac{P_{\max}}{A}. \tag{5}$$

Therefore, it is clear that the accuracy of this analysis depends on the accuracy of the estimation of the

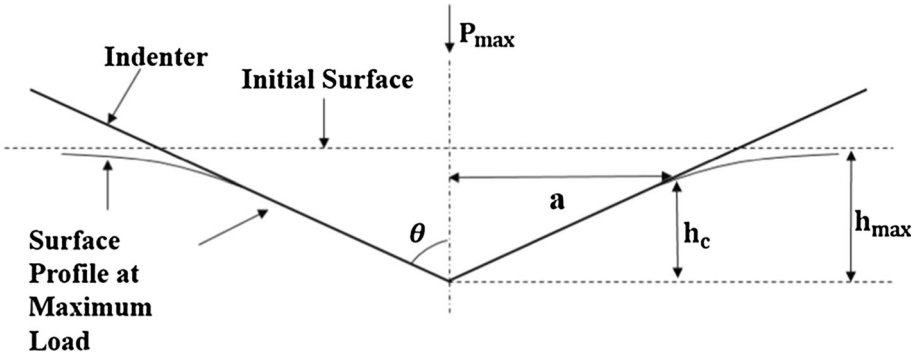


**Figure 2** Illustration of the indentation geometry at maximum force for an ideal conical indenter. Reproduced from [1] with permission from Cambridge University Press.

Poisson's ratio and the measurement of the projected contact area. Actually, the measurement of the projected contact area at the maximum load could be a major source of error because it is challenging to measure accurately in practice, since plastic pile-up or elastic sink-in occurs and affects the size of the real contact area. For example, without considering pile-up, the projected contact area is likely to be underestimated, leading to an overestimated elastic modulus and hardness according to Eqs. (2) and (4). Although the influence of pile-up on measuring the contact area is only significant for materials exhibiting a relatively small amount of elastic recovery after unloading, i.e. $h_f/h_{max} > 0.7$, where $h_f$ is the final indentation depth after unloading and $h_{max}$ is the maximum indentation depth [38]. This analytical approach assumes an elastic-perfectly plastic bulk material. This means that the important work-hardening behaviour of most alloys and metals cannot be taken into account. Also, it is not generally applicable to thin films and coatings on substrate materials.

## Load–displacement relationship—analytical predictions

Regarding the elastoplastic indentation load–displacement curve, there have been theoretical studies providing predictions with known mechanical properties. Solutions for the specific cases of cylindrical and conical indenters were given for the case of an elastic solid by Love [39, 40] based on the general solution of this elastic contact problem proposed by Boussinesq [41]. This is an important development because it brought the relevant theoretical studies to practical applications for the first time. A procedure for deriving analytical predictions of the load–displacement curves for an arbitrary axisymmetric shaped indenter was given by Harding and Sneddon [42, 43]. Figure 2 shows a schematic illustration of indentation for a conical indenter and the relevant quantities. The relationship between the contact depth $h_c$ and the total indentation depth $h$ is given by [43]

$$h = \frac{\pi}{2}h_c = \frac{\pi a}{2\tan\theta} \tag{6}$$

where $\theta$ is the indenter angle and $a$ is the contact radius. It is indicated that the ratio of the contact depth to the indentation depth is a constant, $\frac{\pi}{2}$. It should be noted that the case of material pile-up is not taken into consideration in this expression. In the case of material pile-up, the contact depth could be larger than the indentation depth. The expression for the load is given by [37]

$$P = \frac{\pi}{2}\frac{E}{(1-\nu^2)}\frac{a^2}{\tan\theta}. \tag{7}$$

Combining Eqs. (6) and (7):

$$P = \frac{2E\tan\theta}{\pi(1-\nu^2)}h^2. \tag{8}$$

For a given indenter angle $\theta$ and material properties $E$ and $\nu$, the $P$–$h$ curve of an indentation process can be predicted. Sneddon's analytical prediction has been compared to FE simulations as shown in Fig. 3 [44]. Good agreements have been achieved between the FE simulation and analytical prediction when the same boundary conditions are applied. This analytical procedure is only applicable to the case of a semi-infinite solid contact problem and therefore cannot be applied to indentations on coatings. Another assumption is that the material is elastic-perfectly plastic. Therefore, work hardening is not taken into consideration. This undermines its applicability to most engineering materials, for which work hardening is an important part of the post-yield behaviour.

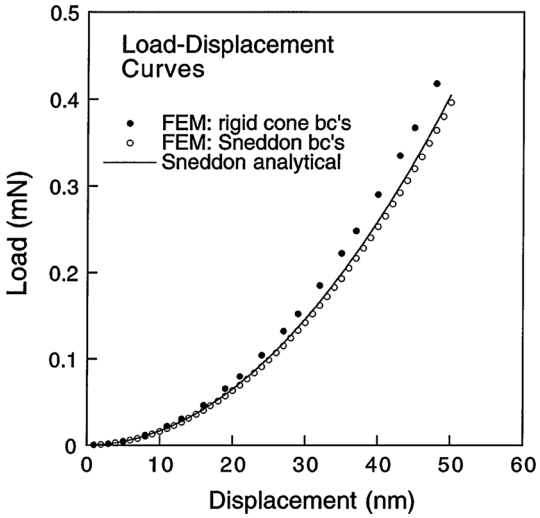


**Figure 3** Load–displacement curves predicted by FE simulation and Sneddon analytical prediction [44].

Malzbender et al. [45, 46] also established analytical predictions of $P$–$h$ curves for nano-indentation. The general expression for the $P$–$h$ relationship is given by

$$P = \frac{E_r h^2}{\left[\frac{1}{\sqrt{\pi}\tan\theta}\sqrt{\frac{E_r}{H}} + \frac{\varepsilon}{\beta}\sqrt{\frac{\pi}{4}}\sqrt{\frac{H}{E_r}}\right]^2} f(n)^2 \quad (9)$$

where $H$ is the hardness, $\varepsilon$ is a geometric constant, ($\varepsilon = 0.72$ for conical indenter), $E_r$ is the reduced elastic modulus, $\beta$ and $f(n)$ are correction functions considering non-rigid indenter and the effect of pile-up and sink-in, respectively. For a conical indenter with indenter angle $\theta \leq 60^\circ$, $\beta$ is given by

$$\beta = 1 + \frac{2(1-2\nu)}{4(1-\nu)\tan\theta} \quad (10)$$

$f(n)$ is given by

$$f(n) \approx (1.28) - (0.8n)\left(1 - \frac{14.78Y}{E_r}\right) \quad (11)$$

where $n$ is the strain-hardening coefficient and $Y$ is the yield strength. Compared to Sneddon's expression, this solution involves empirical constants. It also requires more material property inputs. On the other hand, it is more realistic since it is able to model an imperfect indenter tip and the effect of pile-up and sink-in is taken into consideration.

Very few analytical studies have provided characterisation of the radial displacement profile of the surface region in contact [47]. This prediction depicts a surface in contact in a slightly different shape from the conical indenter. The expression of the radial displacement is given by

$$u = \frac{(1-2\nu)}{4(1-\nu)}\frac{r}{\tan\theta}\left[In\frac{r/a}{1+\sqrt{1-(r/a)^2}} - \frac{1-\sqrt{1-(r/a)^2}}{(r/a)^2}\right] \quad (12)$$

where $r$ is the radial coordinate. Combined with the boundary conditions, this expression is able to describe the shape of the deformed surface completely. Figure 4 [44] shows the comparison between the analytical prediction of the contact surface profile and the results from FE simulation. There is a clear difference when the indenter is simulated as a rigid body, but good agreements have been achieved when it is modelled using the boundary conditions from Sneddon's solution. This analytical prediction could be used as an alternative method of verification for similar FE modelling.

## Indentation experiments

### Indentation range

For the discussion of indentation tests, it is important to clarify the definition of the indentation range, since it could be ambiguous in some studies. According to the ISO 14577 definition [48], the instrumented indentation tests are divided into three ranges: (1) macro-range: $2\ \text{N} \leq F \leq 30\ \text{kN}$; (2) micro-range: $F < 2\ \text{N}$; $h > 0.2\ \mu\text{m}$; and (3) nano-range: $h \leq 0.2\ \mu\text{m}$.

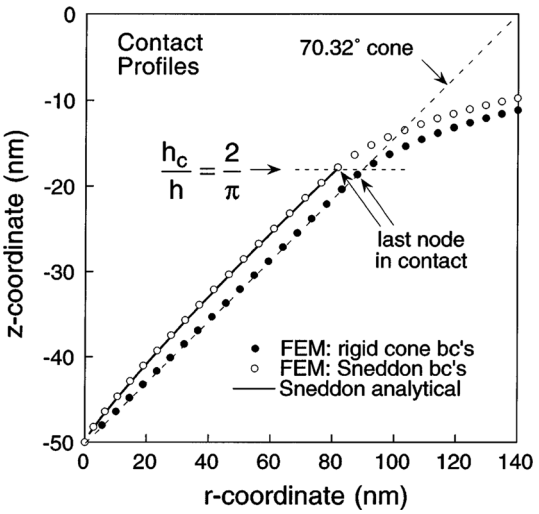


**Figure 4** Surface profiles predicted by FE simulation for two sets of boundary conditions [44].

In this review, this definition is adopted to classify the experiments in the literature. Some of the experimental studies conducted in the literature are in the nano-range, mostly with bulk materials, e.g. [1–3, 5]. Others are in the micro-range, e.g. [6–13, 34]. Experiments have been conducted with coatings on substrates, e.g. [10–13, 34, 35, 49]. Very few indentation experiments have been performed in the nano-range with coatings, e.g. [35].

## Instrumentation

Generally, most instrumented indentation systems consist of an indenter, a displacement sensor and a frame for holding the sample. This type of system is illustrated in Fig. 5 [1]. There are some commercially available systems developed by different companies (such as MTS Systems Corp., Hysitron, Inc., Micro Materials Ltd., CSIRO and CSM Instruments). Regarding certain features, there are some differences between these systems. For example, some of the devices have a vertical indenter axis (MTS Nano Instruments, Hysitron, CSIRO and CSM Instruments systems), while it is horizontal in the Micro Materials system. The other major difference is the method of applying force and measuring displacement. In the MTS Nano Instruments, Micro Materials, CSIRO and CSM Instruments systems, force application and displacement measurement are conducted separately, in different ways. In the Hysitron system, these two processes are performed by the same transducer at the same time [49].

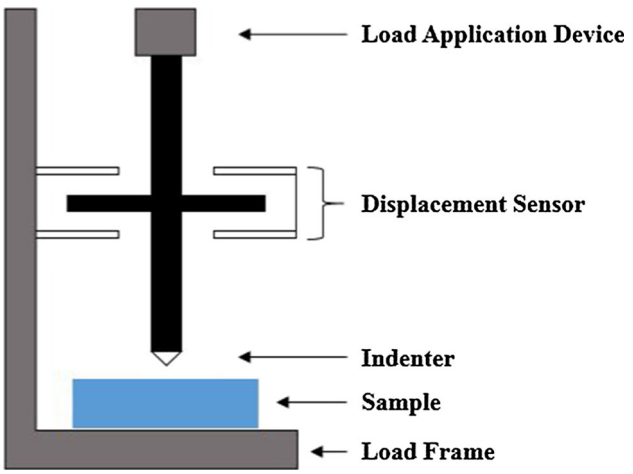


**Figure 5** Schematic illustration of a typical instrumented indentation system. Reproduced from [1] with permission from Cambridge University Press.

## Indenters

There are three main types of indenters used in experiments: spherical, Berkovich and Vickers indenters. Geometries of the Berkovich and Vickers indenter are shown in Figs. 6 and 7. The effects of using different indenter geometries have been investigated in a few studies using FE analysis and experiments, e.g. [50, 51]. A spherical indenter allows the observation of purely elastic deformation changing to elastic–plastic deformation since the initial part of the loading process is within the elastic regime [52–54]. Also, spherical indenters are easier to control so that the substrate effects can be avoided or reduced compared to the sharp indenters, because they penetrate less with the same loading force. Another type of a less sharp indenter is the Knoop indenter, which is suitable for material characterisation in narrow areas, e.g. the cross section of thin films, and studying the direction-dependent properties due to its elongated geometry [55, 56]. It is also useful for indentation of brittle materials since it is less sharp and achieves a 30% lower indentation depth compared to the sharp indenters [51].

## Measurement methods and typical results

There are two types of indentation instruments regarding the feedback control system: force

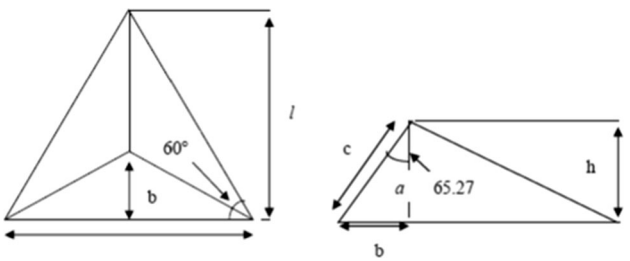


**Figure 6** Berkovich indenter geometry.

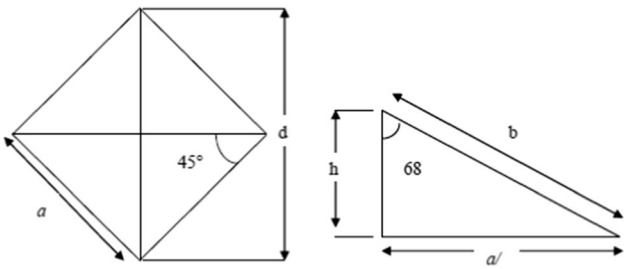


**Figure 7** Vickers indenter geometry.

controlled or displacement controlled. Most indentation systems work as force-controlled process due to the convenience, though displacement-controlled process is applied for some specialised research instruments [49]. However, it should be noted that the displacement is usually a more important parameter to be considered during the indentation process for coated systems. The depth of indentation is a vital concern if the coating layer behaviour needs to be investigated independently from the substrate material. The force and displacement history can be controlled with the signal feedback. Force–displacement curves of bulk materials (copper and glass) and a coated system (copper film on glass substrate) are shown in Figs. 8 and 9, respectively [6]. To compare these data with bulk materials and coated systems, it can be seen that the force–displacement responses of the coated system are generally somewhere between the data of two different bulk materials, reflecting the combined effects. For example, as shown in Figs. 8 and 9, during the loading process at the displacement of 100 nm, the force is about 3 mN for the copper and 6 mN for the glass while it is about 4 mN for the coated system [6].

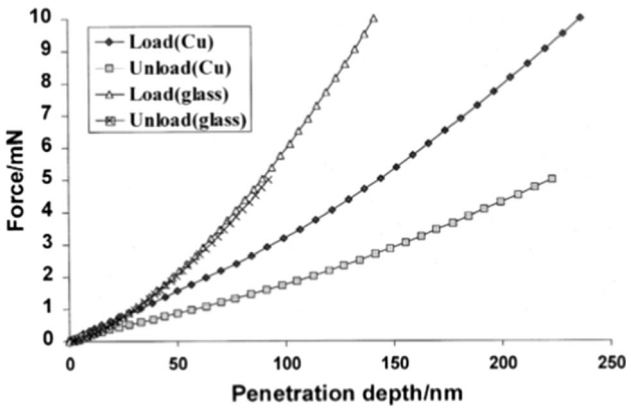


**Figure 8** Force–displacement curve for load–partial unload cycle of copper and glass substrates [6].

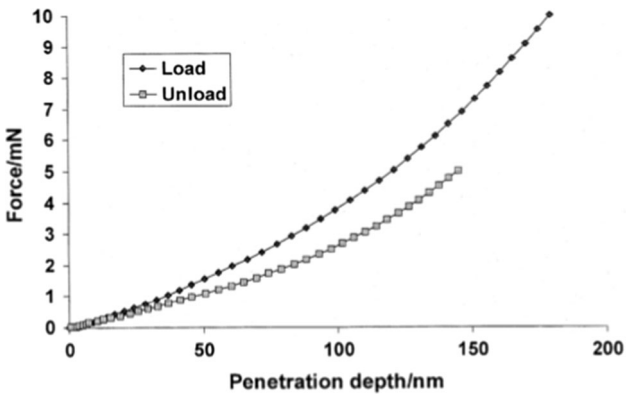


**Figure 9** Force–displacement curve for load–partial unload cycle of 240-nm-thick copper film on a glass substrate [6].

One way to simplify the measurement method is applying a constant loading rate for the force-controlled indentation or a constant displacement rate for a displacement-controlled indentation. The use of a constant loading or displacement rate means that the feedback is no longer necessary [49].

## Finite element modelling

The FE method (FEM) has been a prevalent technique used for studying the field of indentation testing in recent decades, e.g. [3–13]. Generally, good agreements have been achieved between different FE models and experiments. When comparing the prediction made by the FE models and the data obtained from real experiments, usually the calculated Young's modulus, hardness and the force–displacement curves obtained through the indentation process are targeted.

In the field of indentation tests, FE modelling has been mainly used for two purposes: (1) simulating actual experiments and obtaining relevant data of interest for further analysis or acting as an alternative data source, e.g. to obtain the force–displacement curves for the determination of elastoplastic material properties, e.g. [26–28]; (2) conducting parametric studies with similar FE models, i.e. to investigate the effects of some factors of influence in the indentation system, e.g. [9, 13, 50].

The numerical approach certainly has the advantages of reduced time consumption and financial cost, especially for the investigations of the effects of some systematic parameters. It is relatively more convenient to change parameters such as material properties, load and boundary conditions and indenter shape. However, it also has some limitations. For example, it is very difficult to include all realistic details, such as the indenter imperfections, the plasticity models of the materials and the film bonding behaviour for coating systems.

### Typical model definitions and assumptions

FE models have been developed using commercially available software packages, such as ABAQUS or

ANSYS. Most FE indentation models are built using axisymmetric elements, e.g. [3–10]; a few of them employed 3D elements, e.g. [2, 24, 26, 29]. The indenter is usually defined as a perfectly sharp rigid body, meaning that the deformation and blunting of the indenter tip is neglected. Although deformable indenters have been modelled in some studies [46, 50], there is no significant difference in terms of accuracy when it is compared to the FE models with a rigid indenter. Also, the friction between the indenter and the sample surface is assumed to be zero in most cases, as it has been pointed out that the friction has negligible effects on the indentation behaviour. The material test piece is usually defined as fixed in the bottom surface. The loading and unloading processes of the indentation test can be modelled using load control or displacement control. The latter one is more straightforward since displacement control gives direct control over the indentation scale (micro-indentation or nano-indentation). Regarding the simulation of coated systems, the load is usually controlled such that the indentation depth does not exceed 10% of the film thickness so that the indentation is within the limit of critical ratio of coating thickness to indentation depth [30]. This helps to target the coating layer more independently from the substrate material. In a coated system, the coating layer is usually assumed to be perfectly bonded to the substrate layer for the simplicity of simulation. A typical FE model of an indentation test for bulk material is presented in Fig. 10. Regarding the mesh of the FE model, as indicated in Fig. 10, refined meshing is usually presented in the vicinity of the indenter tip because it is the area of interest due to the expected high stress gradients.

There have been some attempts to develop more realistic FE models for this scenario. For example, the friction between the indenter and the sample surfaces has been taken into account in some studies, e.g. [2, 12, 57, 58]. It is discovered that considering the existence of friction leads to a lower amount of pile-up [2], which agrees with the idea of Begley et al. [58] that friction prevents the sliding of material on the sides of the indenter, thus reducing the amount of pile-up. It should be noted that the effects of friction between the indenter and the sample are mainly on the strain distribution and the fracture behaviour. Regarding the determination of material properties, which is mostly about obtaining the load–displacement curves, the influence of contact friction during the indentation is limited. Piana et al. [13] also considered the intrinsic stresses resulting from the thermal residual stresses due to the cooling process from the film deposition temperature to room temperature. These factors are worth considering when the attention is on the test of in-service material samples.

For the definition of material properties in FE models, elastoplastic materials are assumed usually. Also power law strain hardening is considered in most studies since it is a very important plastic behaviour for most materials, especially metals. The viscoplasticity of a material (Zr-based metallic glass) has been taken into consideration by Su and Anand [3]. The viscoplastic behaviour is insignificant at room temperature for most metals and alloys, but they could become important at a higher

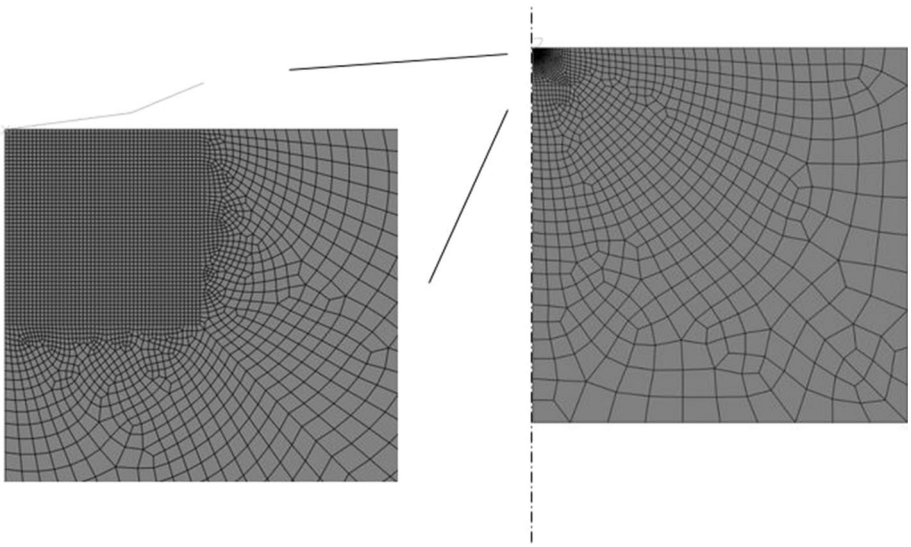

**Figure 10** An axisymmetric FE model with spherical indenter.

temperature, i.e. above approximately one-third of the absolute melting point. Therefore, viscoplasticity is worth considering if the scenario is to perform an indentation test or simulation for a material test piece operating at that high temperature. Otherwise, this factor can be neglected for simplicity to reduce the calculation cost.

## Typical outputs

As mentioned earlier, FE modelling is an important method of an alternative data source to verify or examine the experimental indentation results. Actually, many studies include both experimental data and numerical simulations so that they can be compared to evaluate their validity. Some comparison of load–displacement curves and deformation profiles between experimental data and numerical predictions obtained for indentation on Ni–Co with a spherical indenter is presented in Fig. 11 [7]. There are some inherent dissimilarities between experiments and simulations. The imperfection and deformation of a real indenter tip are usually unknown, but it is usually assumed as perfectly rigid in simulations. Also the contact friction is usually assumed to be zero in FE simulations. These intrinsic differences result in some expected differences between experimental and simulated indentation data as seen in Fig. 11.

Another type of study is the investigation of the effects of certain parameters in the indentation system. The effects of normalised coating yield strength on the indentation response of a coated system are shown in Fig. 12 [59]. Three different normalised coating yield strengths are used in the simulation. This can be done conveniently by changing two input parameters with a verified FE model while it could take much more time and work to perform a series of experiments. Other similar investigations include the parametric study of indenter geometry [50].

The indentation technique has also been applied in other various material-related studies. For example, the strain-rate sensitivity has been investigated by many researchers using indentation techniques, e.g. [60–63]. Figure 13 shows the results of a sensitivity study on the load–displacement responses of nanocrystalline Ni and Ni with larger grain sizes [60]. The nanocrystalline Ni shows a higher sensitivity to the strain rate, since it gives clearly distinct load–displacement curves for different strain rates as shown in Fig. 13b. The transition in the deformation mechanism has been studied by applying nano-indentation tests to both nanograined and coarse-grained stainless steel, showing that the nanograined structure is much more sensitive to the strain rate [63]. The phenomenon of sudden displacement jump observed during the indentation tests on single crystals, or the pop-in effect, has been studied regarding the microstructure of the material, e.g. the stress-induced dislocation nucleation, see e.g. [64, 65].

## Interpretation of indentation data

Indentation tests have been used to measure the hardness of materials for a long time. In recent decades, the need for a more fundamental understanding of indentation data has driven the development

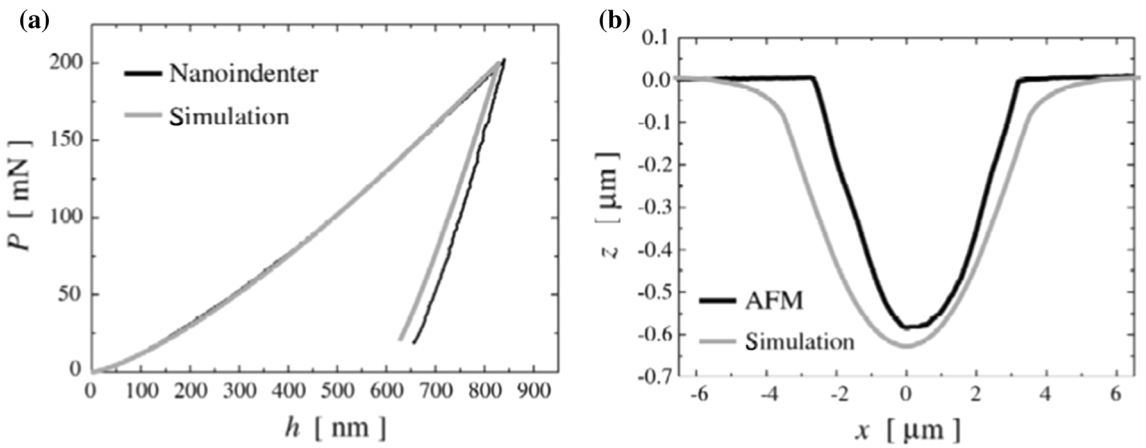


**Figure 11** **a** Comparison between experimental and simulated indentation on Ni–Co with a spherical tip. **b** Comparison between surface deformation profiles of spherical indentation obtained by AFM measurement and FE simulation [7].

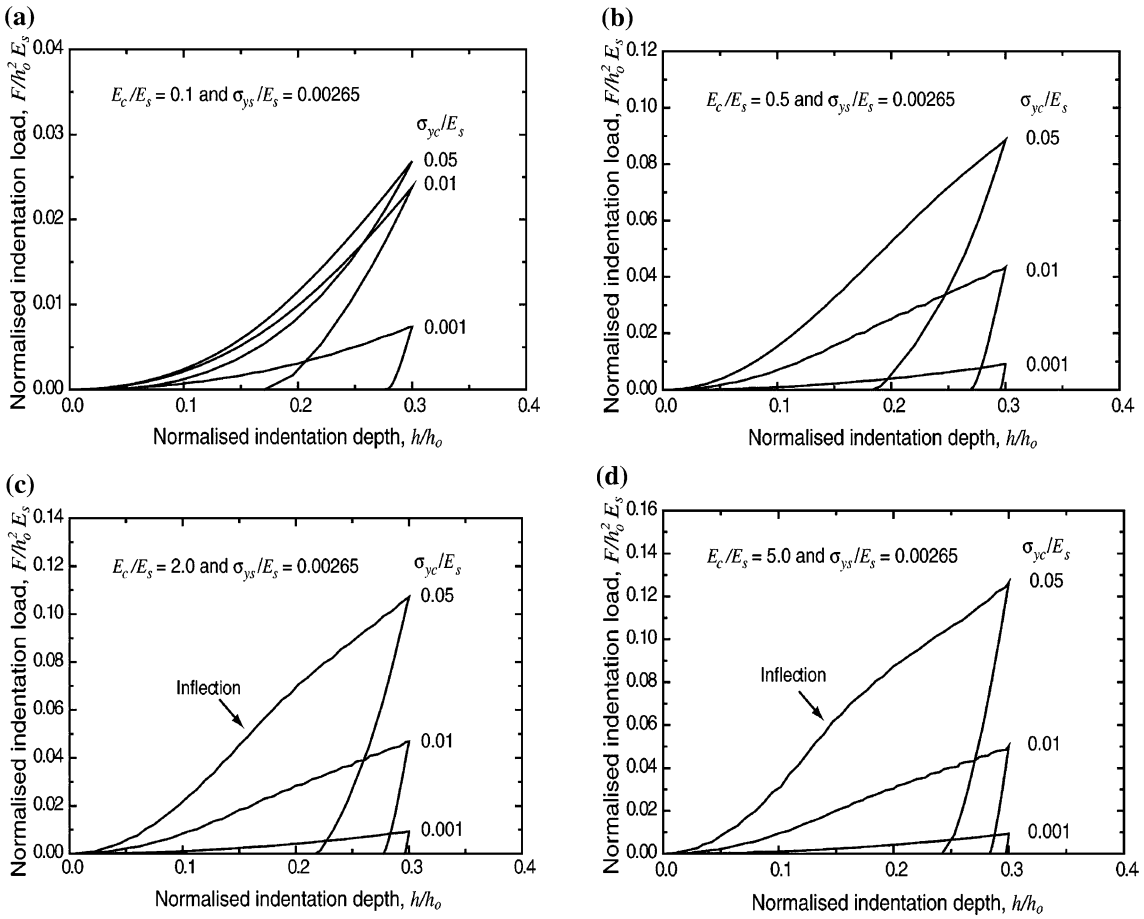


**Figure 12** Effect of normalised coating yield strength ($\sigma_{yc}/E_s$) on the indentation response for a substrate with $\sigma_{ys}/E_s = 0.00265$ and elastic mismatch (Ec/Es) of **a** 0.1, **b** 1.0, **c** 2.0 and **d** 5.0 [59].

of interpretation methods to determine the mechanical material properties, such as elastic modulus, yield strength and work-hardening exponent. Various approaches have been proposed to interpret the data obtained from indentation tests, i.e. the load–displacement data. Generally, these proposed methods can be categorised into three types: (1) dimensional analysis, e.g. [26, 28, 66–69], (2) forward and reverse analysis using FEA, e.g. [7, 24, 25] and (3) analysis using trained neural network, e.g. [70].

## Dimensional analysis

Dimensional analysis has been a common method of extracting the elastic–plastic material properties in many studies, e.g. [26, 28, 66–69, 71]. The dimensionless functions directly relate the material properties to the indentation response. A series of studies have been conducted by Cheng and Cheng [66–68]. This method is based on the assumption of power law plasticity, which can be described as follows,

$$\sigma = \begin{cases} E\varepsilon, & \text{for } \sigma \le \sigma_y \\ R\varepsilon^n, & \text{for } \sigma \ge \sigma_y \end{cases} \tag{13}$$

where $R$ is a strength coefficient. Plastic behaviour of many engineering metals can be closely described by this power law approximation. Generally, the principles of the dimensional analysis can be described as follows. First, the dependent variable is selected and all independent variables and parameters are identified with independent dimensions. Then relationships among dimensionless quantities are established since dimensionless quantities are formed. During the loading process, the loading force F and the indentation depth h are dependent variables. The loading force depends on Young's modulus ($E$),

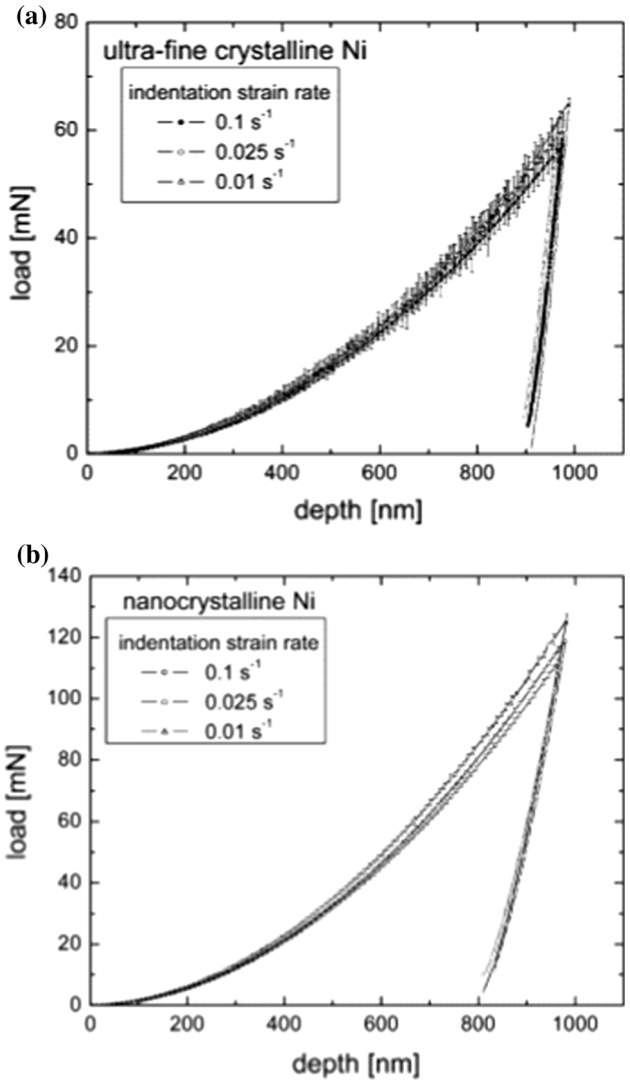


**Figure 13** Load–displacement ($P$–$h$) curves of the **a** ufc Ni (320 nm grain size) and **b** nc Ni (40 nm grain size). The average curve including *error bars* (95% confidence interval) of 10 and 5 curves, respectively, at three different indentation strain rates [60].

Poisson's ratio ($v$), initial yield stress ($Y$), work-hardening exponent ($n$) and the angle of indenter face ($\alpha$). The load $F$ for the loading curve is given by

$$\mathrm{F} = f_L(E, v, Y, n, h, \alpha). \tag{14}$$

Applying the $\pi$ theorem,

$$F = Eh^2\pi_\alpha\left(\frac{Y}{E}, v, n, \alpha\right) \tag{15}$$

where $\pi_\alpha = \frac{F}{Eh^2}$, $v$, $n$ and $\theta$ are dimensionless. The load $F$ depends on $h^2$.

The contact depth $h_c$ can be expressed as

$$h_c = h\pi_\beta\left(\frac{Y}{E}, v, n, \alpha\right). \tag{16}$$

The maximum indentation depth $h_m$ is added during unloading. Now the load $F$ during unloading can be expressed as

$$F = f_U(E, v, Y, n, h, h_m, \alpha). \tag{17}$$

Dimensional analysis gives

$$F = Eh^2\pi_\alpha\left(\frac{Y}{E}, \frac{h}{h_m}, v, n, \alpha\right) \tag{18}$$

where $E$, $Y$, $v, n, \alpha$ are constants. Therefore, the load F depends on $h^2$ and $\frac{h}{h_m}$.

The initial unloading slope $\frac{dF}{dh}$ at $h = h_m$ is expressed as

$$\frac{dF}{dh} = Eh_m\pi_\delta\left(\frac{Y}{E}, v, n, \alpha\right) \tag{19}$$

where the initial unloading slope is proportional to the maximum indentation depth.

The relationship described by Eqs. (15) and (18) can be further investigated by FE analysis. The relationship between experimental variables can be tested with the assistance of these scaling relationships, meaning that potentially a better insight into the indentation in elastic–plastic materials can be obtained. A typical method for extracting mechanical properties from indentation data is constructing dimensionless functions with the concept of a representative strain.

## Representative strain

The concept of representative strain was introduced by Atkins and Tabor [72]. The choice of representative strain is based on the objective of normalising the dimensionless function used in the analysis, which means ensuring that the dimensionless functions are independent of the work-hardening exponent. A definition of representative strain has been made by Dao et al. [26]. The ratio between the constant of Kick's law and the representative stress ($C/\sigma_r$) is related as a function of the ratio between the reduced Young's modulus and the representative strain ($E_r/\sigma_r$) by one of the dimensionless functions proposed [26]. The dimensionless function $\pi_1$ is given by

$$\frac{C}{\sigma_r} = \pi_1\left(\frac{E_r}{\sigma_r}, n\right). \tag{20}$$

The above equation depends on the work-hardening exponent n. It is found, with simulations of a conical indenter, that the dependence on work-hardening becomes negligible for a representative strain $\varepsilon_r$ of 0.033 [26]. This value is also validated by other researchers [73] despite a slight influence in the Young's modulus values. A value of 0.042 is suggested based on a trial-and-error FE analysis using a Vickers indenter [73]. The slight difference can be related to the different methodologies and the friction effect, which is not considered by Dao et al. [26]. A representative strain of 0.037 is found by Casals and Alcala [74] using the same methodology as Dao et al. with a Vickers indenter. It implies that indenter geometry probably has a limited influence on the representative strain value. The representative strain is modified by Ogasawara et al. [28, 69] for a Berkovich indenter to achieve a better physical background and a wider range of material properties. The representative strain and stress are defined as follows [28]

$$\varepsilon_r \equiv \varepsilon_a^p = \varepsilon_a - \varepsilon_a^e \tag{21}$$

$$\sigma_r = R\left(2\varepsilon_a^e + 2\varepsilon_r\right)^n \tag{22}$$

where $\varepsilon_a$ is the equi-biaxial strain, $\varepsilon_a^e$ and $\varepsilon_a^p$ are the elastic and plastic equi-biaxial strain, respectively. They are obtained from equi-biaxial loading with $\sigma_1 = \sigma_2 = \sigma_a$, $\sigma_3 = 0$ $\varepsilon_1 = \varepsilon_2 = \varepsilon_a$, $\varepsilon_3 = -2\varepsilon_a$. $\sigma_1$, $\sigma_2$, $\sigma_3$, $\varepsilon_1$, $\varepsilon_2$ and $\varepsilon_3$ are the components of principal stress and principal strain. In the case of a Berkovich indenter, the representative strain is 0.0115 [28]. The relationship between the dimensionless functions can be obtained numerically using FE analysis. With the defined representative strain and the fitting relationship, material properties can be extracted. The method of dimensional analysis using representative strain avoids measuring the contact area, which is challenging in practice. However, it involves complex dimensionless functions and requires numerical simulations for the forward and inverse analysis. Compared to using Oliver and Pharr method [1], the need for measuring the contact area is avoided by introducing the representative strain, $\varepsilon_r$ and the corresponding representative stress, $\sigma_r$ into the dimensional analysis.

## Inverse analysis using FE techniques

Forward and inverse analysis using FE simulations is another method for extracting material properties from indentation data. The general procedures are [48]: (1) an FE model is built and validated, (2) the model is implemented using certain properties, (3) an inverse or iteration algorithm is constructed, (4) the algorithm is used combined with FE analysis to obtain indentation responses, and finally (5) with reference to the targeted indentation data, material properties can be extracted iteratively by finding the converged FEA simulated indentation. This method is flexible for different indenter geometries and different material models. On the other hand, due to the possible large number of iterations, the computing cost is considerable. Also, for the iteration analysis, an initial guess of the material properties is indispensable, which sometimes could lead to convergence difficulties. Kang et al. [25] proposed a method using FE analysis combined with optimisation algorithms, claiming that elastoplastic properties can be extracted from a single indentation curve without the use of dimensional analysis and representative strain. The applicability of this approach is validated for bulk materials with acceptable accuracy, but further investigation is required for coated systems, in which the indentation depth needs to be controlled within a small range to minimise the effects from the substrate.

## Neural network

A trained neural network is an alternative method of extracting material properties from indentation data. Artificial neural networks are used as a tool to solve complex inverse problems in computational mechanics. The training process is done by carrying out a great number of forward analysis using numerical simulations with the material properties of interest as input [75]. The constructed and trained neural network should then be verified by a new set of FE analysis different from the training set. Huber et al. [70, 76] developed a neural network to determine the constitutive properties of power law materials. The neurons forming the neural network are connected with links to a highly parallel structure. Generally, multiple inputs are fed into each neuron and a single output is obtained. The training process is carried out by implementing a large number of computations, i.e. a large number of input sets are given to the neural network and the outputs are compared to the desired results to compute the error. The neural network is taught to identify the relationship between input and

output data by minimising the error using a back-propagation algorithm to adjust the links between the neurons [76]. A sketch of the multilayer feed forward neural net is shown in Fig. 14 where $x_i$ represents the input values, $y_l$ represents the output values and $w_{ij}$ represents the links between the neurons [70].

This method has the advantages of the capability of including time-dependent properties and obtaining a unique solution for many types of materials, and robust indentation behaviour against experimental error [75]. Also, the network works as a black box system, and since it requires little expertise in FE analysis by the user, it can be implemented by non-FE specialists. On the other hand, it is a time-consuming process, including construction, training and testing of neural networks.

## The uniqueness of extracting material properties from indentation

Indentation tests have been used to investigate the mechanical properties of work-hardening materials, such as Young's modulus, yield strength, Poisson's ratio and work-hardening exponent. The most important indentation data used are the load–displacement curve obtained from an indentation test. However, it has been found that almost identical load–displacement curves can be obtained by combinations of different elastoplastic properties [30, 67, 68, 77] due to the self-similarity [49]. This issue of uniqueness has been addressed systematically by Chen et al. [77]. It has been shown that even with a duel indenter method there are indistinguishable 'mystical' material siblings [77], which have different mechanical properties but give almost identical load–displacement curves. Explicit procedures for finding the mystical materials are established, and alternative methods of distinguishing the mystical materials are proposed [77].

Yet, the mechanics and physics behind the mystical materials require further studies. An indentation technique that always provides a unique solution of the material properties using an indentation response is still needed. Regarding the indentation experiments, the inevitable experimental measurement errors and the material heterogeneity also make it difficult to obtain unique material properties for a given test material. An alternative approach which includes all possible solutions for the plasticity of the material has been proposed considering the experimental errors [78].

## Mechanical characterisation of coated systems by indentation tests

The performance of the coated systems generally depends on the elastic and plastic properties of the coatings. In order to determine the mechanical properties of coatings and to evaluate the conditions of the coated system, indentation testing can be used as a viable method. This section includes the review of experimental research, FE modelling and data interpretation of indentation test on coated systems.

### Experimental research on indentation on coated systems

For indentation tests performed on a coating system, there are more factors of influence to consider

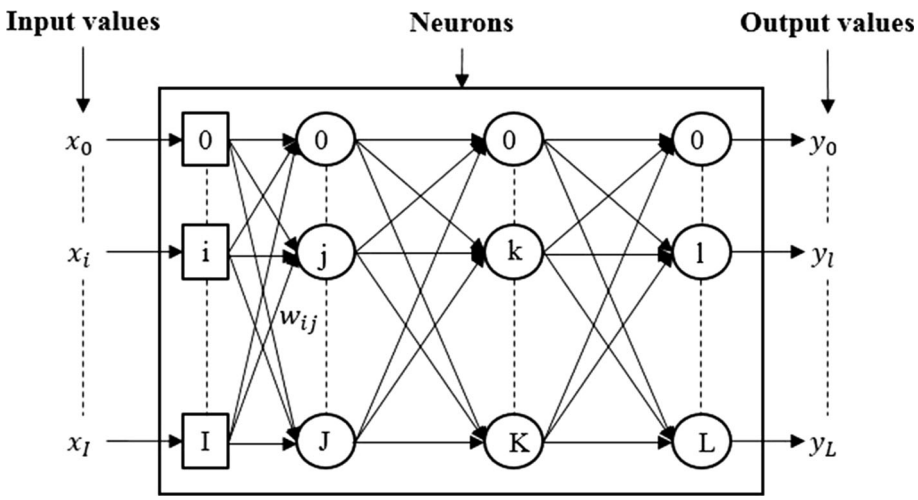


**Figure 14** Sketch of a multilayer feed-forward neural net. Reproduced from [70] with permission from Elsevier.

compared to indentation tests on single bulk materials, such as the indentation depth, indentation size effect and surface conditions, such as the porosity and defects. This extra complexity mainly comes from the small coating thickness and the possible substrate effects. Some test method guidelines have been given by ISO 14577 [79] for single coating layers under the conditions where the substrate effects are not significant and where those effects are detected. Surface preparation should be minimised in order to reduce the possibility of affecting the indentation responses [79]. Surface roughness is an important factor to consider since the thickness of the coating is usually small and the allowed indentation depth is even smaller, which means the test results can be greatly affected by a rough surface within a very small penetration depth. The roughness Ra value, which represents the arithmetical average roughness calculated from the surface peaks and valleys from the mean line over the sampling length, should be less than 5% of the maximum indentation depth if possible [79]. To keep the roughness within an acceptable limit, a polishing process might be necessary. However, for metals, the residual stress and the work-hardening state can be changed by the mechanical polishing process. Stress induced during polishing should be removed. Different models have been proposed to account for the influence of roughness and defects. The Proportional Specimen Resistance (PSR) model developed by Li and Bradt [80] allows the separation of the roughness effect, but it could not take into account the indentation size effect satisfactorily since the relevant parameter is greatly influenced by the presence of roughness [36]. A model proposed by Chicot et al. [81] has been applied to characterise the indentation size effect and to obtain the hardness and the elastic modulus of a porous coating with good agreement achieved with values in the literature [81]. This relationship used for correction is given as follows:

$$P = 26.43 \times \left( HM_0^2 + \frac{H_{LSF}^2}{h_i - h_0} \right)^{\frac{1}{2}} \times (h_i - h_0)^2 \qquad (23)$$

where $HM_0$ is the dynamic Martens macro-hardness, $H_{LSF}$ is the hardness-length-scale factor representing the indentation size effect of the material, $h_i$ is the current indentation depth and $h_0$ is the depth shift. A lower value of hardness is given by this model when the indentation size effect is taken into account by the hardness-length-scale factor [81]. There are a few experimental studies of indentation on coated system, e.g. [11–13, 34–36]. These investigations are mostly aimed at one or two particular coating materials for a single layer of coating. More combinations of different materials for coatings and substrates and the case of multiple layer coated systems may be investigated in future experimental research.

## Finite element modelling of indentation on coated systems

Indentation tests on coated systems have been simulated using FE analysis by many investigators, e.g. [82–89]. For simplicity, most studies have used an axisymmetric model with a conical indenter for the simulation. A fine mesh is used for the coating layer and a coarse mesh is used for the substrate since the indentation penetration only occurs within this layer. Figure 15 shows a typical FE model of an indentation test on a coated system. Generally, perfect adherence between the coating and substrate is assumed for simplicity in the FE models in the literature. This means that no delamination occurs between the coating and substrate, although that could be a possible mode of failure for a coated system. Very few studies have included FE analysis of indentations on coated systems with multiple layers as shown in Fig. 16 [84].

## Determination of mechanical properties of coatings

Compared to the numerous studies on extracting the mechanical properties of bulk materials from indentation data, there are only few studies, e.g. [74, 85, 90–99], providing general solutions to determine the elastoplastic properties of coatings.

### *Dimensional analysis*

Dimensional analysis has been used to extract mechanical properties for coating systems, e.g. [74, 90]. As presented by Tunvisut et al. [74], the loading process of the indentation on a coated system can be described by a functional relationship between the load force F and a series of material properties and parameters as follows

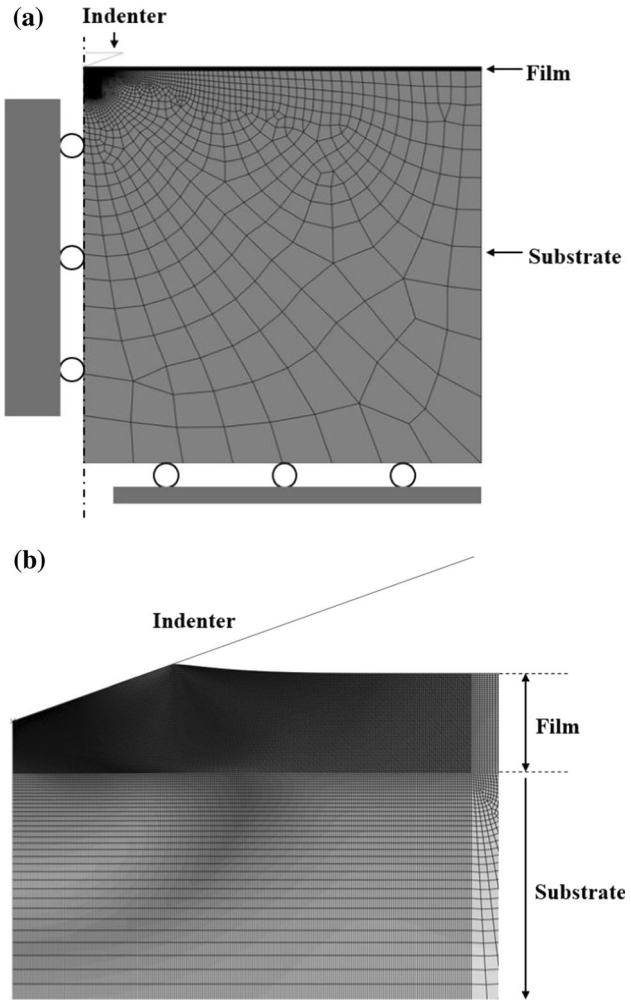


**Figure 15** **a** FE mesh and boundary conditions, **b** details of the mesh in the region near the tip of the indenter during the loading stage.

$$F = F_{\mathrm{L}}\left(E_{\mathrm{c}}, \sigma_{yc}, \nu_{\mathrm{c}}, n_{\mathrm{c}}, E_{\mathrm{s}}, \nu_{\mathrm{s}}, h, h_0, \theta\right) \tag{24}$$

where the subscript c and s stand for coating and substrate, respectively, and $h_0$ is the coating thickness.

With the assumption of knowing the substrate and coating thicknesses, the Buckingham π theorem can be applied for normalisation as follows

$$\frac{F}{h_0^2 E_{\mathrm{s}}} = \prod_{\alpha}\left(\frac{h}{h_0}, \frac{E_{\mathrm{c}}}{E_{\mathrm{s}}}, \frac{\sigma_{yc}}{E_{\mathrm{s}}}, \nu_{\mathrm{c}}, \nu_{\mathrm{s}}, n_{\mathrm{c}}, \theta\right). \tag{25}$$

Similarly, the unloading process is expressed as follows

$$F = F_{\mathrm{U}}\left(E_{\mathrm{c}}, \sigma_{yc}, \nu_{\mathrm{c}}, n_{\mathrm{c}}, E_{\mathrm{s}}, \nu_{\mathrm{s}}, h, h_0, h_{\mathrm{m}}, \theta\right) \tag{26}$$

where $h_{\mathrm{m}}$ is the maximum indentation depth. Dimensional analysis of the above relationship gives

$$\frac{F}{h_0^2 E_{\mathrm{s}}} = \prod_{\beta}\left(\frac{h}{h_0}, \frac{h_{\mathrm{m}}}{h_0}, \frac{E_{\mathrm{c}}}{E_{\mathrm{s}}}, \frac{\sigma_{yc}}{E_{\mathrm{s}}}, \nu_{\mathrm{c}}, \nu_{\mathrm{s}}, n_{\mathrm{c}}, \theta\right). \tag{27}$$

Considering the initial unloading slope, the derivative of $\prod_{\beta}$ with respect to $\frac{h}{h_0}$ can be obtained as follows

$$\frac{1}{h_0 E_{\mathrm{s}}}\frac{\mathrm{d}F}{\mathrm{d}h}\bigg|_{h=h_{\mathrm{m}}} = \prod_{\delta}\left(\frac{h_{\mathrm{m}}}{h_0}, \frac{E_{\mathrm{c}}}{E_{\mathrm{s}}}, \frac{\sigma_{yc}}{E_{\mathrm{s}}}, \nu_{\mathrm{c}}, \nu_{\mathrm{s}}, n_{\mathrm{c}}, \theta\right). \tag{28}$$

The functional relationships described by Eqs. (25) and (28) can be quantified using numerical analysis. From FEM analysis, the relationship shown in Eqs. (28) is calibrated as follows [90]

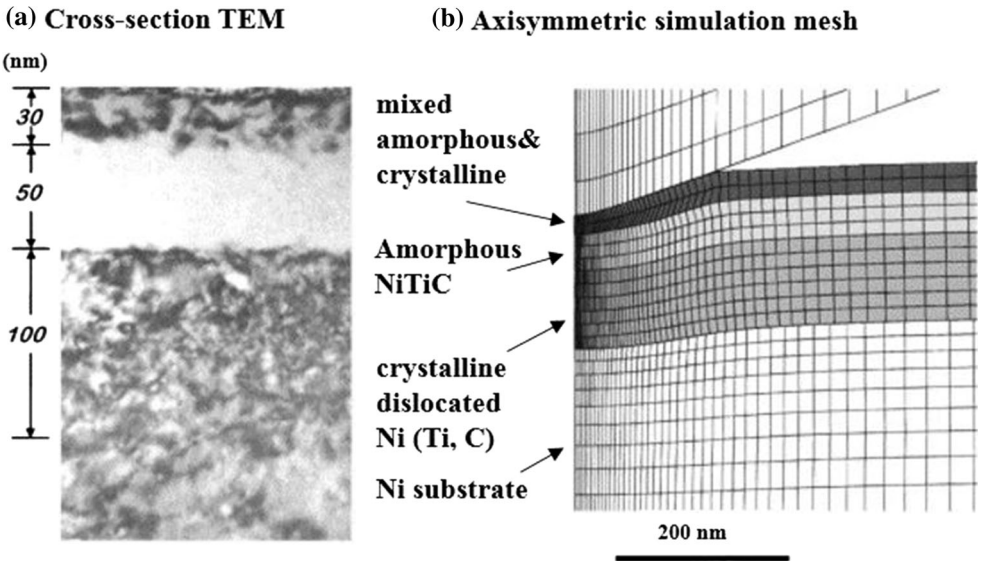


**Figure 16** **a** *Bright-field*, cross-sectional TEM image of Ni implanted with Ti and C. **b** Axisymmetric FE mesh used to model the sample in (**a**), shown during a simulation with the indenter at maximum penetration. The *grey areas* mark the three layers with different assigned properties in the simulations. Reproduced from [84] with permission from Elsevier.

$$\left.\frac{1}{h_0 E_s}\frac{dF}{dh}\right|_{h=h_m} = \begin{cases} 2.1\left(\frac{E_c}{E_s}\right)^{0.86}, & \frac{E_c}{E_s} \le 1, \\ -7\left(\frac{E_c}{E_s}\right)^{-0.32} - 27.1\left(\frac{E_c}{E_s}\right)^{0.01} + 13.9\left(\frac{E_c}{E_s}\right)^{0.002} + 22.3, & \frac{E_c}{E_s} \ge 1, \end{cases} \quad (29)$$

The general method of extracting the mechanical properties is finding the best match of the indentation curves describing the relationships between the normalised parameters obtained from the experimental tests and the numerical simulations. This approach of data interpretation can easily determine the Young's modulus with an acceptable 10% error for a work-hardening coating material. However, it is suggested [74] that an additional measurement of the final contact area is needed to tackle the issue of uniqueness for the determination of yield strength and work-hardening exponent, because it has been found that almost identical normalised load–displacement curves can be obtained for materials with different combinations of yield strength and work-hardening exponent. This issue can limit the applicability of this interpreting method since accurately measuring the contact area is challenging in practice. The assumption that the properties of the substrate material are known in advance is sometimes not appropriate in a real situation when the information regarding substrate material may be limited. The other issue is that the indentation is performed to a depth of 33% of the coating thickness in the studies of Tunvisut et al. [74, 90] while other studies report that the critical ratio of indentation depth to film thickness to separate the coating behaviour from the substrate effects is about 10% [59, 82, 100].

### *Analytical solutions*

Analytical solutions have been proposed to predict the indentation response of coatings and have been used to extract the mechanical properties of the coating materials [91–96]. These analytical solutions, with formulae given in Refs. [94–96], allow the stresses and deformations under a spherical indenter to be calculated. Good agreements have been achieved by comparisons between the analytical calculations, FE analysis and experiments [91–93]. However, the extraction of material properties is limited to elastic properties, such as Young's modulus, since the plastic properties are not covered by these analytical solutions. Comparison between different analytical models might provide a better insight, but no other analytical solutions for plastic behaviour have been seen in the literature.

### *FE method*

Numerical simulation is another important method to extract material properties for coatings. An iterative FE technique was used by Knapp [83] to determine the Young's modulus and yield stress. Young's modulus and the yield stress are varied, while Poisson's ratio and the work-hardening exponent are fixed. Generally, the iterative procedures are aimed at finding a good fit to the experimental load–displacement curve. This method, however, does not attempt to extract the work-hardening exponent, which is important in many engineering materials. The uniqueness of the material property combination obtained in this study has not been discussed. When more mechanical properties are considered, the issue of uniqueness usually needs further investigation. Also, the computational work is expensive due to the iterative process involved. Tang and Arnell [87] also proposed a method to extract Young's modulus and hardness based on FEA. By introducing mathematical models involving the thickness index, defined as the coating thickness to indenter radius, the stiffness ratio, defined as the ratio of coating to substrate Young's modulus, and the hardness ratio, defined as the ratio of coating to substrate yield stress, the proposed method is able to extract Young's modulus and the hardness of the coating from the load–displacement data without expensive iterative computational work. Yet the hardening behaviour is not considered. The introduced parameter, i.e. the ratio of coating thickness to indenter radius, limits this method to be applied only to indentation tests with a spherical indenter.

Another method based on FE analysis involves a parametric study and measuring the size of the plastic zone [34]. The objective is to find the best fit of both the load–displacement curve and the plastic zone size simultaneously. Because of the need for measuring the plastic zone size, a larger indentation depth is preferred for a better identification and measurement. However, in the case of a thin film on a substrate, increasing the indentation depth raises a

challenge in the separation of the indentation response of the coating layer from the substrate. Ma et al. proposed a hybrid method based on FE analysis to determine the yield strength and strain-hardening exponent. The work-hardening exponent is related to a characteristic parameter, defined based on the load–displacement curve and then related to the yield stress and the maximum load [85]. The main limitation of this method is the involvement of empirical equations.

## Other investigations on coated system subjected to indentation

There are some studies conducting investigations on coated systems subjected to indentation, including the critical ratio of coating thickness to indentation depth and the substrate effects from coated systems, see e.g. [59, 82, 88, 89, 101–104]. These studies are important because one major challenge for the mechanical characterisation of coated systems is separating the indentation response of the coating from the coating–substrate system.

### *Critical ratio of coating thickness to indentation depth*

In the case of indentation on a coated system, there is a critical value of maximum indentation depth that should not be exceeded in order to minimise the effects of the substrate. When the indentation depth is larger than this critical value, the indentation response is a mixture of coating and substrate responses, making it difficult to extract single material properties when the interest is on the coating. Traditionally, the indentation depth is limited to less than 10% of the film thickness in order to measure the film properties [59, 82, 100]. However, this value could be inappropriate for certain combination of coating and substrate materials. The critical ratio of thickness to indentation depth has been related to the yield strength ratio of coating to substrate and the indenter tip radius by deriving an empirical equation [82] given by

$$R_{2\%} = a_0 + a_1\left(\frac{Y_c}{Y_s}\right) + a_2\left(\frac{Y_c}{Y_s}\right)^2 + a_3\left(\frac{Y_c}{Y_s}\right)^3 \quad (30)$$

where the constants $a_0$, $a_1$, $a_2$ and $a_3$ are functions of the radius of the round indenter tip (an imperfect conical indenter tip). $R_{2\%}$ is the critical ratio of thickness to indentation depth at which the substrate has negligible effect (<2%). The critical ratio increases when the yield strength ratio is increased. The critical ratio also increases significantly when the indenter tip deviates from a perfect shape even slightly [82]. A similar methodology is also used by Busso and Gamonpilas [59]. This empirical equation gives an approximate guide for the critical ratio when the yield strength ratio and indenter tip radius are known to be within certain ranges. It also suggests that the assumption of a perfect indenter tip should be examined carefully in the case of an indentation on a coating. The sensitivity of the critical ratio is verified in another study [101].

### *Substrate effects*

The effects of the substrate on the indentation behaviour of coated systems have been investigated [59, 100]. Different coating/substrate systems have been studied experimentally [100], such as a soft coating on a hard substrate and a hard coating on a soft substrate. The substrate has noticeable effects on the measured coating hardness in the case of a hard coating on soft substrate since the substrate is more likely to deform even at small indentation [100]. This effect is negligible when the coating is much softer than the substrate because the substrate deformation is minor. Similar conclusions have been made in another study [59], where the effects of substrate properties on the indentation behaviour of coated systems are investigated using dimensional analysis combined with FE analysis. In the case of a small coating to substrate yield strength ratio, i.e. $\frac{\sigma_{yc}}{\sigma_{ys}} < 1$, the indentation depth can exceed 30% of the film thickness while it decreases to 5% in the case of a hard coating on a soft substrate, i.e. $\frac{\sigma_{yc}}{\sigma_{ys}} > 10$ [59]. It indicates that indentation depth should be applied with more caution for the coated systems consisting of a hard coating and a soft substrate.

## Conclusions

The present work provides a review of mechanical characterisation using indentation tests with the focus on coated systems. The relevant theoretical background, experimental work, numerical simulations and data interpretation methods have been reviewed for single bulk materials. The discussion on

bulk materials is extended to cover the mechanical characterisation of coated systems. The extra factors for consideration during experimental testing on coated systems, such as surface preparation, roughness and indentation size effect, have been identified and discussed.

Most FE modelling of indentations on coated systems in the literature uses axisymmetric model with a conical indenter for simplicity. Very few studies have included modelling of indentation on a coated system with multiple layers. A few proposed methods of extracting mechanical properties of thin films and coatings have been reviewed, including dimensional analysis, analytical models and FE inverse analysis. Generally, the existing methods are applicable within certain limitations. A universally effective method to extract a unique set of power law elastic and plastic properties, i.e. Young's modulus, yield strength, Poisson's ratio and work-hardening exponent, of coatings from indentation data is still needed. Some effective interpretation methods devised for indentation on bulk materials are worthy of further investigation, such as the optimisation algorithms used for forward and inverse analysis, to see whether these methods can be extended for coated systems.

The fact that the substrate material can easily influence the indentation response obtained for a coated system usually makes it difficult to determine the mechanical properties of the coating material independently, because more variables are introduced into the system. This issue leads to the requirement of a better understanding of substrate effects and the critical ratio of coating thickness to indentation depth at which the influence of substrate starts to take effect. In addition, a comprehensive parametric study would be beneficial to investigate the factors influencing the indentation of coated systems and to obtain an insight into the indentation behaviours systematically. For future experimental research, it is recommended that a wider range of coating–substrate mismatch and multiple coating layers is investigated.

## Acknowledgement

This work was supported by the Engineering and Physical Sciences Research Council (EPSRC) through EPSRC Centre for Doctoral Training in Innovative Metal Process (IMPaCT, www.impact.ac.uk) [Grant Number EPL016206].

## Compliance with ethical standards

**Conflict of interest** The authors declare that they have no conflict of interest.

## References

[1] Oliver WC, Pharr GM (1992) An improved technique for determining hardness and elastic modulus using load and displacement sensing indentation experiments. J Mater Res 7:1564–1583

[2] Vaidyanathan R, Dao M, Ravichandran G, Suresh S (2001) Study of mechanical deformation in bulk metallic glass through instrumented indentation. Acta Mater 49:3781–3789

[3] Su C, Anand L (2006) Plane strain indentation of a Zr-based metallic glass: experiments and numerical simulation. Acta Mater 54:179–189

[4] Zhang J, Niebur GL, Ovaert TC (2008) Mechanical property determination of bone through nano- and micro-indentation testing and finite element simulation. J Biomech 41:267–275

[5] Misra RDK, Venkatsurya P, Wu KM, Karjalainen LP (2013) Ultrahigh strength martensite-austenite dual-phase steels with ultrafine structure: the response to indentation experiments. Mater Sci Eng A 560:693–699

[6] Olofinjana AO, Bell JM, Jamting AK (2000) Evaluation of the mechanical properties of sol–gel-deposited titania films using ultra-micro-indentation method. Wear 241:174–179

[7] Stauss S, Schwaller P, Bucaille JL, Rabe R, Rohr L, Michler J, Blank E (2003) Determining the stress-strain behaviour of small devices by nanoindentation in combination with inverse methods. Microelectron Eng 67–68:818–825

[8] Hu Y, Shen L, Yang H, Wang M, Liu T, Liang T, Zhang J (2006) Nanoindentation studies on nylon 11/clay nanocomposites. Polym Testing 25:492–497

[9] Harsono E, Swaddiwudhipong S, Liu ZS, Shen L (2011) Numerical and experimental indentation tests considering size effects. Int J Solids Struct 48:972–978

[10] Karimzadeh A, Ayatollahi MR, Alizadeh M (2014) Finite element simulation of nano-indentation experiment on aluminum 1100. Comput Mater Sci 81:595–600

[11] Kot M, Rakowski W, Lackner JM, Major Ł (2013) Analysis of spherical indentations of coating-substrate systems: experiments and finite element modeling. Mater Des 43:99–111

[12] Li W, Huang C, Yu M, Liao H (2013) Investigation on mechanical property of annealed copper particles and cold sprayed copper coating by a micro-indentation testing. Mater Des 46:219–226

[13] Piana LA, Pérez REA, Souza RM, Kunrath AO, Strohaecker TR (2005) Numerical and experimental analyses on the indentation of coated systems with substrates with different mechanical properties. Thin Solid Films 491:197–203

[14] Venkateswaran P, Xu ZH, Li X, Reynolds AP (2009) Determination of mechanical properties of Al–Mg alloys dissimilar friction stir welded interface by indentation methods. J Mater Sci 44:4140–4147. doi:10.1007/s10853-009-3607-4

[15] Monclus MA, Young TJ, Di Maio D (2010) AFM indentation method used for elastic modulus characterization of interfaces and thin layers. J Mater Sci 45:3190–3197. doi:10.1007/s10853-010-4326-6

[16] Okayasu M, Takasu S, Mizuno M (2012) Relevance of instrumented nano-indentation for the assessment of the mechanical properties of eutectic crystals and α-Al grain in cast aluminum alloys. J Mater Sci 47:241–250. doi:10.1007/s10853-011-5791-2

[17] Zhu LN, Xu BS, Wang HD, Wang CB, Yang DX (2011) Measurement of mechanical properties of 1045 steel with significant pile-up by sharp indentation. J Mater Sci 46:1083–1086. doi:10.1007/s10853-010-4876-7

[18] Cheng W, Wang M, Xu C, Zhang J, Liang W, You B, Nie K (2015) Microstructure characterization and indentation hardness testing behavior of Mg–8Sn–xAl–1Zn alloys. J Mater Sci 30:1043–1048. doi:10.1007/s11595-015-1270-y

[19] Nakayama T, Sakaue K, Ogawa T, Kobayashi Y, Teratani T (2009) Evaluations of mechanical properties of DLC film by indentation method and the effect of substrate. Zairyo J Soc Mater Sci 58:833–840

[20] Bhushan B, Kulkarni AV, Bonin W, Wyrobek JT (1996) Nanoindentation and picoindentation measurements using a capacitive transducer system in atomic force microscopy. Philos Mag A 74:1117–1128

[21] Newey D, Wilkins MA, Pollock HM (1982) An ultra-low-load penetration hardness tester. J Phys E Sci Instrum 15:119–122

[22] Bell TJ, Bendeli A, Field JS, Swain MV, Thwaite EG (1992) The determination of surface plastic and elastic properties by ultra micro-indentation. Metrologia 28:463–469

[23] Randall NX, Consiglio R (2000) Nanoscratch tester for thin film mechanical properties characterization. Rev Sci Instrum 71:2796–2799

[24] Kang JJ, Becker AA, Sun W (2012) determining elastic-plastic properties from indentation data obtained from finite element simulations and experimental results. Int J Mech Sci 62:34–46

[25] Kang JJ, Becker AA, Sun W (2013) Determination of elastic and viscoplastic material properties obtained from indentation tests using a combined finite element analysis and optimization approach. Proceedings of the Institution of Mechanical Engineers, Part L: Journal of Materials: Design and Applications 229:1–14

[26] Dao M, Chollacoop N, Van Vliet KJ, Venkatesh TA, Suresh S (2001) Computational modeling of the forward and reverse problems in instrumented sharp indentation. Acta Mater 49:3899–3918

[27] Zhao M, Ogasawara N, Chiba N, Chen X (2006) A new approach to measure the elastic–plastic properties of bulk materials using spherical indentation. Acta Mater 54:23–32

[28] Ogasawara N, Chiba N, Chen X (2006) Measuring the plastic properties of bulk materials by single indentation test. Scripta Mater 54:65–70

[29] Antunes JM, Menezes LF, Fernandes JV (2006) Three-dimensional numerical simulation of Vickers indentation tests. Int J Solids Struct 43:784–806

[30] Luo J, Lin J, Dean TA (2006) A study on the determination of mechanical properties of a power law material by its indentation force–depth curve. Phil Mag 86:2881–2905

[31] Gamonpilas C, Busso EP (2007) Characterization of elastoplastic properties based on inverse analysis and finite element modeling of two separate indenters. J Eng Mater Technol 129:603–608

[32] Luo J, Lin J (2007) A Study on the determination of plastic properties of metals by instrumented indentation using two sharp indenters. Int J Solids Struct 44:5803–5817

[33] Le MQ (2008) A Computational study on the instrumented sharp indentations with dual indenters. Int J Solids Struct 45:2818–2835

[34] Farrissey LM, McHugh PE (2005) Determination of elastic and plastic material properties using indentation: development of method and application to a thin surface coating. Mater Sci Eng A 399:254–266

[35] Rico A, Gómez-García J, Múnez CJ, Poza P, Utrilla V (2009) Mechanical properties of thermal barrier coatings after isothermal oxidation. Surf Coat Technol 203:2307–2314

[36] Łatka L, Chicot D, Cattini A, Pawłowski L, Ambroziak A (2013) Modeling of elastic modulus and hardness determination by indentation of porous yttria stabilized zirconia coatings. Surf Coat Technol 220:131–139

[37] Fischer-Cripps AC (2006) Critical Review of analysis and interpretation of nanoindentation test data. Surf Coat Technol 200:4153–4165

[38] Pharr GM, Oliver WC, Brotzen FR (1992) On the generality of the relationship among contact stiffness, contact

area, and elastic-modulus during indentation. J Mater Res 7:613–617

[39] Love AEH (1929) The stress produced in a semi-infinite solid by pressure on part of the boundary. Philos Trans R Soc Lond Ser A Contain Pap Math Phys Character 228:377–420

[40] Love AEH (1939) Boussinesq's problem for a rigid cone. Q J Math 10:161–175

[41] Boussinesq J (1885) Applications des Potentiels a l'etude de equilibre dt du mouvement des solides elastiques. Gauthier-Villars, Paris

[42] Harding JW, Sneddon IN (1945) The elastic stresses produced by the indentation of the plane surface of a semi-infinite elastic solid by a rigid punch. Math Proc Cambridge Philos Soc 41:16–26

[43] Sneddon IN (1965) The relation between load and penetration in the axisymmetric Boussinesq problem for a punch of arbitrary profile. Int J Eng Sci 3:47–57

[44] Hay JC, Bolshakov A, Pharr GM (1999) A critical examination of the fundamental relations used in the analysis of nanoindentation data. J Mater Res 14:2296–2305

[45] Malzbender J, de With G, den Toonder J (2000) The P-h2 relationship in indentation. J Mater Res 15: 1209–1212

[46] Malzbender J (2002) Indentation load-displacement curve, plastic deformation, and energy. J Mater Res 17:502–511

[47] Sneddon IN (1951) Fourier transforms. McGraw-Hill Book Company, New York, pp 450–467

[48] ISO (2015) ISO 14577-1:2015, Metallic materials—instrumented indentation test for hardness and materials parameters—part 1: test method. ISO, Geneva

[49] Vanlandingham MR (2003) Review of instrumented indentation. J Res Nat Inst Stand Technol 108:249–265

[50] Sakharova NA, Fernandes JV, Antunes JM, Oliveira MC (2009) Comparison between Berkovich, Vickers and conical indentation tests: a three-dimensional numerical simulation study. Int J Solids Struct 46:1095–1104

[51] Zhang J, Sakai M (2004) Geometrical effect of pyramidal indenters on the elastoplastic contact behaviors of ceramics and metals. Mater Sci Eng A 381:62–70

[52] Field JS, Swain MV (1993) A simple predictive model for spherical indentation. J Mater Res 8:297–306

[53] Francis HA (1976) Phenomenological analysis of plastic spherical indentation. ASME J Eng Mater Technol 98:272–281

[54] Le MQ (2012) Material characterization by instrumented spherical indentation. Mech Mater 46:42–56

[55] Riester L, Blau PJ, Lara-Curzio E, Breder K (2000) Nanoindentation with a Knoop indenter. Thin Solid Films 377:635–639

[56] Riester L, Bell TJ, Fischer-Cripps AC (2001) Analysis of depth-sensing indentation tests with a Knoop indenter. J Mater Res 16:1660–1667

[57] Bolshakov A, Pharr GM (1998) Influences of pileup on the measurement of mechanical properties by load and depth sensing indentation techniques. J Mater Res 13:1049–1058

[58] Begley MR, Evans AG, Hutchinson JW (1999) spherical impression of thin elastic films on elastic–plastic substrates. Int J Solids Struct 36:2773–2788

[59] Gamonpilas C, Busso EP (2004) On the effect of substrate properties on the indentation behaviour of coated systems. Mater Sci Eng A 380:52–61

[60] Schwaiger R, Moser B, Dao M, Chollacoop N, Suresh S (2003) Some critical experiments on the strain-rate sensitivity of nanocrystalline nickel. Acta Mater 51:5159–5172

[61] Chen J, Lu L, Lu K (2006) Hardness and strain rate sensitivity of nanocrystalline Cu. Scripta Mater 54:1913–1918

[62] Maier V, Durst K, Mueller J, Backes B, Höppel HW, Göken M (2011) Nanoindentation strain-rate jump tests for determining the local strain-rate sensitivity in nanocrystalline Ni and ultrafine-grained Al. J Mater Res 26:1421–1430

[63] Misra RD, Zhang Z, Jia Z, Venkatsurya PK, Somani MC, Karjalainen LP (2012) Nanoscale deformation experiments on the strain rate sensitivity of phase reversion induced nanograined/ultrafine-grained austenitic stainless steels and comparison with the coarse-grained counterpart. Mater Sci Eng A 548:161–174

[64] Lorenz D, Zeckzer A, Hilpert U, Grau P, Johansen H, Leipner HS (2003) Pop-in effect as homogeneous nucleation of dislocations during nanoindentation. Physical Rev B 67(172101):1–4

[65] Durst K, Backes B, Franke O, Göken M (2006) Indentation size effect in metallic materials: modeling strength from pop-into macroscopic hardness using geometrically necessary dislocations. Acta Mater 54:2547–2555

[66] Cheng YT, Cheng CM (2004) Scaling, dimensional analysis, and indentation measurements. Mater Sci Eng R Rep 44:91–150

[67] Cheng CM, Cheng YT (1999) Can stress–strain relationships be obtained from indentation curves using conical and pyramidal indenters". J Mater Res 14:3467–3473

[68] Capehart TW, Cheng YT (2003) Determining constitutive models from conical indentation: sensitivity analysis. J Mater Res 18:827–832

[69] Ogasawara N, Chiba N, Chen X (2005) Representative strain of indentation analysis. J Mater Res 20:2225–2234

[70] Huber N, Tsagrakis I, Tsakmakis C (2000) Determination of constitutive properties of thin metallic films on substrates by spherical indentation using neural networks. Int J Solids Struct 37:6499–6516

[71] Kang JJ, Becker AA, Sun W (2011) A combined dimensional analysis and optimization approach for determining elastic-plastic properties from indentation tests. J Strain Anal Eng Des 46:749–759

[72] Atkins AG, Tabor D (1965) Plastic indentation in metals with cones. J Mech Phys Solids 13:149–164

[73] Antunes JM, Fernandes JV, Menezes LF, Chaparro BM (2007) A new approach for reverse analyses in depth-sensing indentation using numerical simulation. Acta Mater 55:69–81

[74] Tunvisut K, O'Dowd NP, Busso EP (2000) Use of scaling functions to determine mechanical properties of thin coatings from microindentation tests. Int J Solids Struct 38:335–351

[75] ISO (2008) NPR-ISO/TR 29381, Metallic materials—measurement of mechanical properties by an instrumented indentation test—indentation tensile properties. ISO, Geneva

[76] Huber N, Tsakmakis C (1999) Determination of constitutive properties from spherical indentation data using neural networks. Part ii: plasticity with nonlinear isotropic and kinematic hardening. J Mech Phys Solids 47:1589–1607

[77] Chen X, Ogasawara N, Zhao M, Chiba N (2007) On the uniqueness of measuring elastoplastic properties from indentation: the indistinguishable mystical materials. J Mech Phys Solids 55:1618–1660

[78] Moussa C, Hernot X, Bartier O, Delattre G, Mauvoisin G (2014) Evaluation of the tensile properties of a material through spherical indentation: definition of an average representative strain and a confidence domain. J Mater Sci 49:592–603. doi:10.1007/s10853-013-7739-1

[79] ISO (2007) ISO 14577-4:2016 Metallic materials—instrumented indentation test for hardness and materials parameters—part 4: test method for metallic and non-metallic coatings. ISO, Geneva

[80] Li H, Bradt RC (1993) The microhardness indentation load/size effect in rutile and cassiterite single crystals. J Mater Sci 28:917–926. doi:10.1007/BF00400874

[81] Chicot D, Gil L, Silva K, Roudet F, Puchi-Cabrera ES, Staia MH, Teer DG (2010) Thin film hardness determination using indentation loading curve modelling. Thin Solid Films 518:5565–5571

[82] Sun Y, Bell T, Zheng S (1995) Finite element analysis of the critical ratio of coating thickness to indentation depth for coating property measurements by nanoindentation. Thin Solid Films 258:198–204

[83] Knapp JA, Follstaedt DM, Barbour JC, Myers SM (1997) Finite element modeling of nanoindentation for determining the mechanical properties of implanted layers and thin films. Nucl Instrum Methods Phys Res, Sect B 127–128:935–939

[84] Knapp JA, Follstaedt DM, Myers SM, Barbour JC, Friedmann TA, Ager JW, Monteiro OR, Brown IG (1998) Finite element modeling of nanoindentation for evaluating mechanical properties of MEMS materials. Surf Coat Technol 103–104:268–275

[85] Ma DJ, Xu KW, He JW (1998) Numerical simulation for determining the mechanical properties of thin metal films using depth-sensing indentation technique. Thin Solid Films 323:183–187

[86] Lichinchi M, Lenardi C, Haupt J, Vitali R (1998) Simulation of Berkovich nanoindentation experiments on thin films using finite element method. Thin Solid Films 312:240–248

[87] Tang K (1999) Determination of coating mechanical properties using spherical indenters. Thin Solid Films 355–356:263–269

[88] Panich N, Sun Y (2004) Effect of penetration depth on indentation response of soft coatings on hard substrates: a finite element analysis. Surf Coat Technol 182:342–350

[89] Xu Z, Rowcliffe D (2004) Finite element analysis of substrate effects on indentation behaviour of thin films. Thin Solid Films 447–448:399–405

[90] Tunvisut K, Busso EP, O'Dowd NP (2002) Determination of the mechanical properties of metallic thin films and substrates from indentation tests. Philos Mag A 82:2013–2029

[91] Chudoba T, Schwarzer N, Richter F (1999) New possibilities of mechanical surface characterization with spherical indenters by comparison of experimental and theoretical results. Thin Solid Films 355:284–289

[92] Chudoba T, Schwarzer N, Richter F (2000) Determination of elastic properties of thin films by indentation measurements with a spherical indenter. Surf Coat Technol 127:9–17

[93] Chudoba T, Schwarzer N, Richter F, Beck U (2000) Determination of mechanical film properties of a bilayer system due to elastic indentation measurements with a spherical indenter. Thin Solid Films 377–378:366–372

[94] Schwarzer N, Whittling M, Swain M, Richter F (1995) The analytical solution of the contact problem of spherical indenters on layered materials: application for the investigation of tin films on silicon. Thin Solid Films 270:371–375

[95] Schwarzer N, Richter F, Hecht G (1999) The elastic field in a coated half-space under hertzian pressure distribution. Surf Coat Technol 114:292–303

[96] Schwarzer N, Chudoba T, Billep D, Richter F (1999) Investigation of coating substrate compounds using

inclined spherical indentation. Surf Coat Technol 116–119:244–252

[97] Li JF, Wang XY, Liao H, Ding CX, Coddet C (2004) Indentation analysis of plasma-sprayed Cr3C2-NiCr coatings. J Mater Sci 39:7111–7114. doi:10.1023/B:JMSC.0000047561.79036.82

[98] Shiwa M, Weppelmann E, Munz D, Swain MV, Kishi T (1996) Acoustic emission and precision force-displacement observations of pointed and spherical indentation of silicon and TiN film on silicon. J Mater Sci 31:5985–5991. doi:10.1007/BF01152149

[99] Bressan JD, Tramontin A, Rosa C (2005) Modeling of nanoindentation of bulk and thin film by finite element method. Wear 258:115–122

[100] Saha R, Nix WD (2002) Effects of the substrate on the determination of thin film mechanical properties by nanoindentation. Acta Mater 50:23–38

[101] Chen J, Bull SJ (2009) On the factors affecting the critical indenter penetration for measurement of coating hardness. Vacuum 83:911–920

[102] Sakharova NA, Fernandes JV, Oliveira MC, Antunes JM (2010) Influence of ductile interlayers on mechanical behaviour of hard coatings under depth-sensing indentation: a numerical study on TiAlN. J Mater Sci 45:3812–3823. doi:10.1007/s10853-010-4436-1

[103] Ghosh S, Das S, Bandyopadhyay TK, Bandyopadhyay PP, Chattopadhyay AB (2003) Indentation responses of plasma sprayed ceramic coatings. J Mater Sci 38:1565–1572. doi:10.1023/A:1022997203996

[104] Chiou SY, Gan D (2007) Interfacial mechanical properties of TiN coating on steels by indentation. J Mater Sci 42:2745–2752. doi:10.1007/s10853-006-1362-3